Impact of the polydispersion of TiO_2 materials on their particle size calculated from specific surface area results obtained during an interlaboratory comparison exercise

Sébastien Bau, Sebastien Artous, Sébastien Jacquinot, Dominique Locatelli, Jean-François Hochepied, Nicolas Feltin, Carine Chivas-Joly

Impact of the polydispersion of TiO_2 materials on their particle size calculated from specific surface area results obtained during an interlaboratory comparison exercise

S. Bau [a], S. Artous [b], S. Jacquinot [b], D. Locatelli [b], J-F. Hochepied [c,e], N. Feltin [d], C. Chivas-Joly [d, *]

[a] *INRS, Pollutant Metrology Division, 1 rue du Morvan, 54500 Vandoeuvre les Nancy, France*

[b] *Univ. Grenoble Alpes, CEA, Liten, DTNM, 38000 Grenoble, France*

[c] *Unité de Chimie et Procédés (UCP), ENSTA Paris, Institut Polytechnique de Paris, 91120 Palaiseau, France.*

[d] *LNE, CARMEN Plateform - Nanometrology, 29 Avenue Roger Hennequin, 78197 Trappes Cedex, France*

[e] *Centre des Matériaux, Mines Paris, Université PSL, 91003 Evry*

* Corresponding author:
Carine Chivas-Joly
Email: Carine.chivas-joly@lne.fr
Tel. +33 1 30 69 10 72.

Keywords

size measurement, TiO_2, BET, nanoparticle, Volume Specific Surface-Area

1. Introduction

Nanomaterials (NM) in powder form are used in numerous applications such as buildings, textiles, papers, rubbers, plastics, to cite a few [1-5]. Therefore, inhalation exposure to airborne particles potentially released when handling such powders (bagging, transferring, cleaning, embedding, grinding, or any operation throughout the entire life-cycle of the powders) is possible [6-12]. The first step of any risk assessment strategy is hazard identification; the potential hazards of nanomaterials remain uncertain [13]. Furthermore, whether a material shall be considered a nanomaterial or not a nanomaterial has regulatory consequences [14]. However, to determine whether a material is a nanomaterial or not remains difficult. This is particularly due to the absence of standardized methods to accurately determine the number size distribution of constituent particles, from which the proportion of sub-100 nm

particles shall be used. If this proportion is greater than 50%, the material is a nanomaterial, according to the definition adopted by the European Commission [15].

Implemented in France since 2013, the R-Nano declaration of nanomaterials (only in French, available at https://www.r-nano.fr/?locale=en) also relies on unequivocal identification tools (electron microscopy). However, according to a recent review, the fields relating to the physicochemical characterization of nanomaterials, and in particular the size of constituent particles are not well informed in the database [16].

In response to this lack of harmonized characterization methods [17, 18], the work published by the JRC in 2022 [19] defines a common approach how to identify, through appropriate analyses, whether a material is a nanomaterial or not in the sense of the European Commission definition. It provides recommendations on how to select the appropriate analytical measurement techniques for different types of the materials (e.g. suspension or powder) and the morphology (e.g. size and shape) of the particles, and indicates the steps necessary to classify a material as a nanomaterial or not. Beyond regulation [20], determining the size of constituent particle has applications in risk assessment [21, 22], toxicological [23, 24] or epidemiological studies [25, 26].

Electron microscopy (EM) techniques remain the preferred methods providing information concerning the particle size distribution of constituent particles. Microscopy techniques (AFM, SEM, TEM, etc.) are the only so-called direct techniques for size determination. Indeed, their measurement principle is based on direct observation of the particle, and the measurement obtained is a "geometric" size. The latter can be directly traceable to the unit of length (the meter), provided that the technique is correctly calibrated in an SI-traceable manner. This is why these instruments are powerful metrological tools for the characterization of particle size, size distribution, shape and, in some cases, state of agglomeration. In line with the definition of nanomaterials adopted by the European Commission [15], EM allows the fraction of particles with a diameter less than 100 nm to be determined, even within agglomerates. However, this analytical technique, costly and time-consuming, requires a high level of expertise, and lacks standardized approaches for both sample preparation and particle imaging and analysis. The question of analysing a sufficient number of images in order to have a statistically significant analysis [27] must also be considered. In addition, a potential operator effect of the order of 15% has already been reported [28-30],

Introduced by Kreyling *et al.* [31], Volume Specific Surface-Area ($VSSA$) has been identified by different authors [32-38] as an alternative method to electron microscopy techniques to evaluate particle size of a sample in powder form containing a pure substance, i.e. a population

of particle with a single chemical composition, and under the assumption of monodisperse particles. VSSA has been integrated in the NanoDefine as well as the JRC decision trees as a screening method [14]. VSSA is an indirect or integral technique; its result has no direct link with the unit of length defined in the SI, as it is not a direct observation of the particle. In the vast majority of cases, these methods are capable of analysing a signal emitted or derived from a group of particles present in the sample. With indirect techniques, size measurement results from a calculation or modelling step. Consequently, unlike microscopy techniques, the measurand is not a geometric size, but an equivalent diameter corresponding to an ideal spherical particle with identical optical / electrical properties or aerodynamic behavior to the particle under study [14]. Each technique has its own dimensional measurand (and thus bring complementary information about dimensional characteristics). VSSA is an integral method that provides the equivalent diameter of a sphere whose VSSA is the same than the one of the particle.

For non-porous particulate materials, $VSSA$ corresponds to the surface-to-volume ratio of a powder material. It is determined from the product of the external mass specific surface-area of a powder (SSA), and its skeletal density (ρ):

$$VSSA = SSA \cdot \rho \quad (1)$$

Contrary to EM-based measurements, determining the SSA of a powder sample does not require its dispersion, which reduces other possible artefacts, as stated in Babick *et al.* [35]. Two analytical techniques have to be applied to determine VSSA: gas adsorption (nitrogen, argon or krypton, and application of the well-known BET [39] model or t-plot model [40] in case of porous materials), and helium pycnometry [41-43]. In the definition of nanomaterials adopted by the European Commission [15] in 2022, the VSSA is used as an exclusion criterion allowing materials to be categorized as "non nanomaterials" (VSSA < 6 m^2/cm^3).

In the recent past, Bau *et al.* [43] conducted theoretical and experimental work aimed at accounting for the polydispersion of the constituent particles in order to refine the estimation of the equivalent diameter of the particles estimated from the VSSA. The results obtained on 8 powders showed that taking into account polydispersion (assuming constituent particles follow a normal distribution) makes it possible to refine the associated constituent particle diameter and to approach the measurements made by electron microscopy to within ± 25% [27-30].

In the present paper, we aim to investigate the impact of two parameters on VSSA-based measurements: (i) the polydispersion of the size and (ii) the shape of constituent particles. We have chosen four TiO_2 samples considered to have low porosity, corresponding to particles widely used in consumer products (cosmetic, drug, paint, self-cleaning materials…) and

produced in large volume. Indeed, 10,000 tons of TiO_2 nanomaterials were declared in the French R-nano base in 2021, according to the report on the declarations of substances imported, manufactured or distributed in France. The objectives of this study were:

- To demonstrate inter-laboratory repeatability of specific surface area (SSA) measurements provided by four French laboratories,
- To perform a comparison of the size distributions (mean diameter and standard deviation) of the constituent particles obtained by image analyses from electron microscopy carried out by three partners, considered as the reference,
- To determine the diameter of the constituent particles based on the measured VSSA and accounting for constituent particle polydispersion,
- Ultimately, decide on the use of the VSSA to determine the size of the constituent particles compared to the reference measurement.

2. Materials and methods

2.1. Materials

Four kinds of TiO_2-particles have been investigated with different types of structure (rutile and anatase), with or without surface chemical coating and various morphologies (rod, pseudo-spherical) in powder form (Table 1).

Various sources of titanium dioxide (TiO_2) (nano)particles were chosen: Nano-TiO_2-Rods were synthesized by Mines-Paris, TiO_2-E171 coated SiO_2, mainly used as white colouring agent in the drugstore, was a raw material previously studied [44]. Two industrial grades of titanium dioxide powders were tested: TiO_2-µ-rutile was a commercial paint additive and TiO_2-LSSA was supplied by a French manufacturer.

Table 1. Description of the TiO_2 involved in this interlaboratory comparison [44]

Sample	Description	Crystal structure	Coating
TiO_2 - Rods	Synthetized powder	Anatase	None
TiO_2 - E171	Raw material	Anatase	SiO_2
TiO_2 - µ-rutile	Commercial powder	Rutile	*
TiO_2 - LSSA	Commercial powder	Anatase	*

* Not defined

Each of the four participants received the same batch of material in powder form with the procedure for the sample analysis, whose main parameters have been previously defined between the four institutes. The principal parameters measured were the specific surface area (SSA) from gas adsorption, and the size of constituent particles from electron microscopy. Each partner received TiO_2 in powder form and was responsible for preparing the samples, following a specific protocol consisting of several steps

2.2. Methods

The specific surface area of the samples and the size of constituent particles were measured by BET and SEM, respectively.

As stated in the introduction, results obtained from an indirect (VSSA-based) and a direct (EM) technique are compared in this study. For VSSA, the size of particles was determined by converting the SSA into equivalent diameter ($d_{mean-SSA}$), assuming pure, non-porous and monodisperse particles. This value ($d_{mean-SSA}$) was compared to the equivalent diameter obtained by EM ($d_{mean-EM}$).

2.2.1. Number size distribution of constituent particles from EM

All EM analyses were performed manually, with the aim of measuring the size distribution of particles, according to the counting rule 4 in the work from Bresch *et al.* [45] where isolated particles as well as the constituent particles within agglomerates/aggregates are measured. The TiO_2 involved in this study are constituted by slightly anisotropic particles, except for TiO_2-Rods whose constituent particles present a higher anisotropy. In practice, for the case of nearly spherical particles, the latter $d_{mean-EM}$ is obtained from the projected surface-area (A) of a constituent particle assuming its sphericity:

$$d_{mean-EM} = \sqrt{\frac{4A}{\pi}} \quad (2)$$

This descriptor is also recommended in the work from Bresch *et al.* [45], in particular when the size results measured via EM are compared with results obtained by other methods.

For the TiO_2-Rod sample, the intercomparison of the values between techniques was made by considering the minimum Feret diameter (noted $d_{Feret-min-EM}$ and corresponding to the smallest dimension between two parallel lines tangent to the contour of a particle) obtained with EM and assuming that the VSSA-based equivalent diameter is comparable to the diameter of the rod cross-section, i.e. the smallest dimension.

Each partner received TiO_2 in powder form and was responsible for preparing the samples, following its own protocol, except for TiO_2 E171 sample, which was prepared by LNE and sent directly to the other partners.

At LNE, the different powder samples were suspended in 2 mL ultrapure water (resistivity of 18.2 MΩ.cm) and sonicated during 20 minutes (ultrasonic probe energy 1667 J/mL - 40% amplitude, pulsed mode - 10s ON / 10s OFF) to minimize agglomeration. The recommended protocol for getting a good dispersion of particles on the substrate consists in depositing a drop (7.5 up to 10 µL) of the suspension on a silicon wafer substrate by using a spin-coater to prevent any agglomeration process [46]. SEM images of particles were acquired using a Zeiss ULTRA-Plus field emission (FE) microscope equipped with a GEMINI optical column (Zeiss, Oberkochen, Germany) at LNE. Secondary electron (SE) images were collected with the In-Lens detector integrated in-side the column.

At CEA Grenoble, 10µl of sample were deposited on a piece of Silicon wafer. The liquid sample is left to dry in ambient air (regulated between 18 and 23 °C) and the wafer is then bonded to the In-lens SEM mount. Electron microscopy with energy dispersive X-ray (SEM/EDX) spectroscopy was performed using a Model S-5500 SEM (Hitachi) combined with a Noran EDX system (Thermo Scientific®). Particle thresholding of SEM images was performed using Visilog7® software from Thermo Fisher Scientific Inc®.

At INRS, a few powder is first suspended into isopropanol. Samples for electron microscope observation were prepared following the specific grid-on-drop method [47-49] using TEM copper 400 mesh carbon film grids (reference AGG2400C, Agar scientific, Rotherham, England). Each sample was observed using transmission electronic microscopy (2100F, Jeol, Japan) at an acceleration voltage of 200 kV and with magnifications in the range of 50,000x to 120,000x. Images were acquired using a side-mounted camera (Orius SC200D, Gatan, USA). The particle size distributions were determined using the free software Fiji (Wayne Rasband and Contributors, National Institutes of Health, USA https//imageJ.net).

The images were used to establish the size distribution of the constituent particles in the powder. For each TiO_2 sample, 15 to 20 images were collected.

In the present study, constituent particle size distributions were based on a number of particles counted ranging from 103 to 313. The number of size bins was adjusted for each powder sample, with a minimum of bins equal to $\sqrt[3]{2n}$ [50], n being the larger number of particles observed for each material (249 for TiO_2 E171, 313 for LSSA, 311 for µ-rutile and 249 for rods). The size distributions measured by EM-based analysis were fitted by a normal (gaussian) function, using Origin Pro software (OriginPro, Version 2019b, OriginLab Corporation,

Northampton, MA, USA). The output mean diameter $d_{mean-EM}$ or $d_{Feret-min-EM}$ and standard deviation σ were determined, associated with the 95%-confidence interval for both parameters.

2.2.2. Specific surface area

The analytical system performed in this study was an ASAP 2020 (Micromeritics) for LNE samples, a Belsorp-Max (Bel Japan) for INRS and CEA and ASAP2000 micromeritics BET for Mines. The samples were outgassed a minimum of 24 h under vacuum at 200°C before proceeding to N_2 adsorption experiments [51]. All measurements were performed at 77 K and triplicated. Adsorption/desorption isotherms are plotted with the quantity of gas adsorbed (in cm^3/g) as a function of the relative pressure (P/P_0) over an interval of 0.01 - 0.99 P/P_0. Thanks to the BET method, which has been applied to all TiO_2 samples, an external particles specific surface area can be estimated by working on the linear part of the isotherm for P/P_0 values, generally between 0.05 and 0.3 [52, 53]. The minimum quantity required for measurement was 0.5 grams. Internal standards have been used by each participant for the calibration for its device.

2.2.3. Density

Particle density is involved in the determination of the VSSA of a sample, as stated in Equation 1. Four replicates were used to determine the average powder density of the different samples by Helium pycnometry (Accupyc 1340, Micromeritics) at Mines, which is considered as the reference measurement. The skeletal densities of the powders were also determined by Helium pycnometry by CEA and INRS using another equipment (Belsorp Max, Bel Japan), where the volumetric capacity is measured 10 times by He and reported to the weight of the sample. The temperature of the sample cell is controlled by a water bath at 40°C. All the powders were dried overnight in an oven at 150°C before performing the measurements.

2.2.4. Volume specific surface area (VSSA) and constituent particle diameter

VSSA is an integral measurement method that provides an indirect representation of particle size, noted $d_{mean-SSA}$. Table 2 gathers the expressions of surface area, volume, specific surface area in volume of spherical and cylindrical, monodisperse particles.

Table 2. Expressions of surface area, volume, specific surface area in volume of spherical and cylindrical, monodisperse particles

	Spherical particles	Rod-type particles (assuming $L \gg d$)
SA	πd^2	πdL
V	$\frac{\pi}{6}d^3$	$\frac{\pi}{4}d^2L$
$VSSA = SA/V$	$\frac{6}{d}$	$\frac{4}{d}$

The relationship between the measured volume specific surface area VSSA and the equivalent diameter of the constituent particles, $d_{mean-SSA}$ is:

$$d_{mean-SSA} = \frac{6}{VSSA} \quad (3)$$

for spherical particles, and:

$$d_{mean-SSA} = \frac{4}{VSSA} \quad (4)$$

for rod-type particles. The values of $d_{mean-SSA}$ obtained from VSSA determination (based on SSA and powder density) were compared to the constituent particle diameters measured from EM-images, considered as the reference.

Bau *et al.* [43] introduced a correction factor accounting for constituent particle polydispersion, resulting in the reduction of the VSSA of a sample:

$$\theta = \frac{VSSA_{poly}}{VSSA_{mono}} \ (\theta \leq 1) \quad (5)$$

Under the assumption of a normal distribution of constituent particle size, this approach was also included in this intercomparison.

3. Results and discussion

3.1. Size characterization using electron microscopy (SEM/TEM)

EM is an imaging method to determine to the number-based size distribution of constituent particles even within agglomerates or aggregates. However, it requires a preliminary sample preparation before nanoparticles deposit and analysis. TiO_2 samples were measured by partners to obtain the size distribution of the constituent particles. Fig. 1 illustrates TiO_2-samples SEM images.

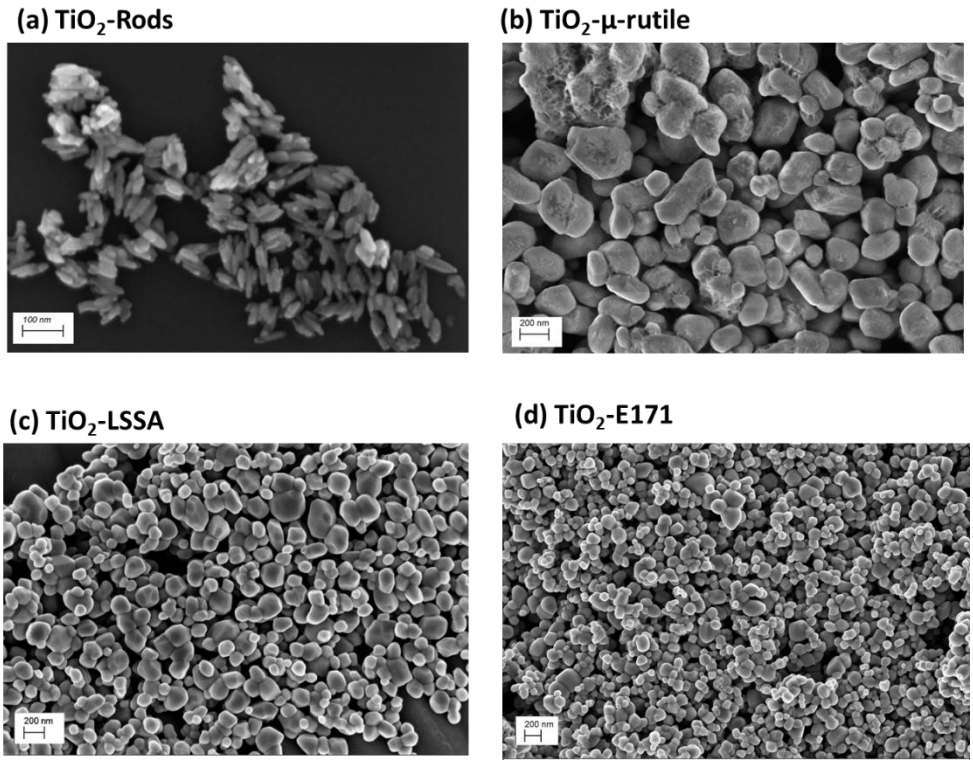

Figure 1. Representative SEM images of all TiO_2 samples (magnification x 100 000 for image a and magnification x 25 000 for images b, c, d)

The selected TiO_2 samples present different morphologies. The three titanium dioxide with the anatase structure seem homogeneous; TiO_2-LSSA (Fig. 1c) and E171 (Fig. 1d) show a quasi-spherical shape, while the TiO_2 Rod (Fig. 1a) has an elongated shape. Finally, the only TiO_2 with a rutile structure (Fig. 1b) appears to be more heterogeneous.

Fig. 2 provides the number-based size distribution histograms built from the analysis of particles ($103 \leq n \leq 313$) assuming the particles are spherical, except for the TiO_2 – rod that presents anisotropy (aspect ratio $L/d \sim 5$, Fig. 1a) and for which the minimum Feret diameter ($d_{Feret-min-EM}$) was extracted.

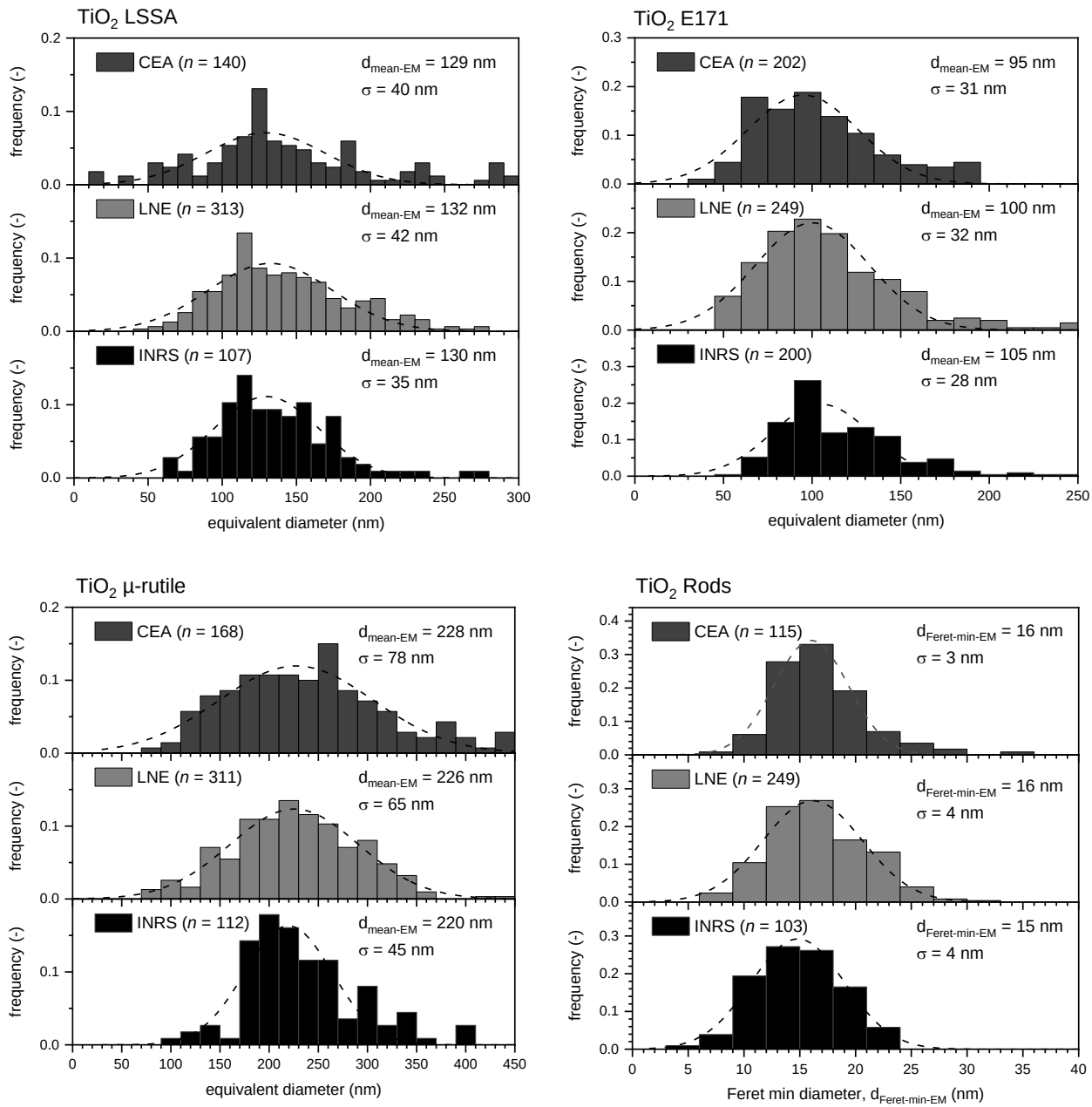

Figure 2. Number size distributions of constituent particles obtained on TiO_2 samples by the three partners. The values indicated in each graph correspond to the mean diameters and standard deviations stemming from the gaussian fits (dash lines).

As shown in Figure 2, the number-based size distributions are polydispersed, whatever the TiO_2 sample considered. A continuous distribution covering a wide range of sizes is observed, indicating the high polydispersity of the constituent particles in the different samples ($\sigma/d_{mean-EM}$ around 30%).

It is therefore legitimate to question the validity of the model based on monodisperse constituent particle size. This motivated the work from Bau *et al.* [43], who state that "This strong hypothesis can be considered far from reality, since materials are typically composed of

polydisperse constituent particles [19, 20]; the latter being potentially either agglomerated or even aggregated within the material."

The mean diameters ($d_{mean-EM}$), and standard deviations (σ) determined from the fitted normal distributions (dashed lines in Fig. 2) are reported in Fig.3 for each laboratory; the uncertainties displayed correspond to the confidence interval of the gaussian fit.

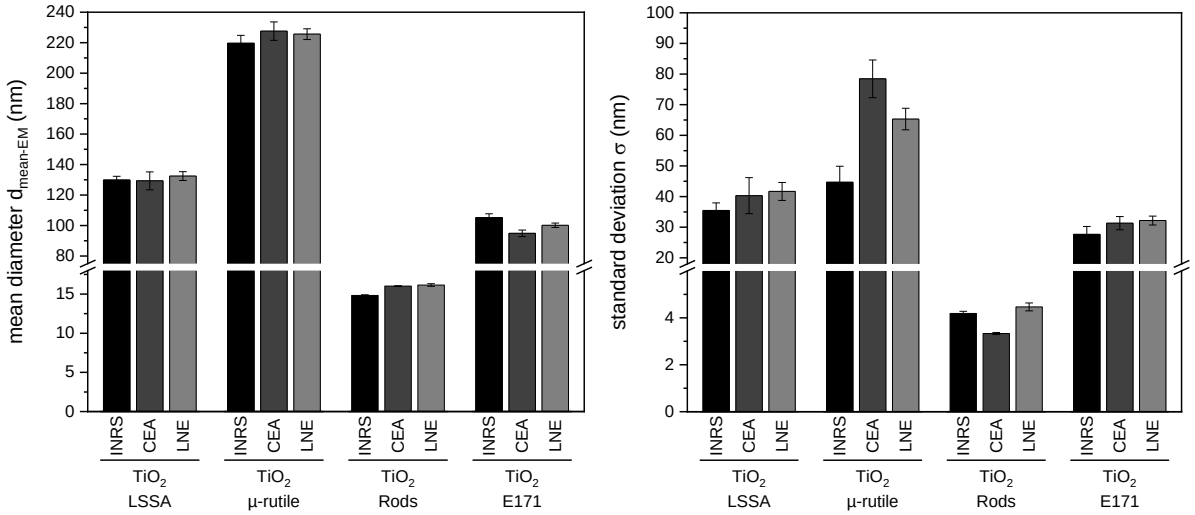

Figure 3. (a) Mean diameters of TiO_2-particles and (b) standard deviations of the size distribution of TiO_2 samples

The mean diameter of constituent particles lies just around the threshold of 100 nm for TiO_2-E171. For TiO_2-rods, the minimum Feret diameter of particles is largely smaller than 100 nm (Fig. 3(a)) such that this material is qualified as NM according to EC definition [15]. For TiO_2-LSSA and TiO_2-µ-rutile, the size is significantly greater than 100 nm.

The $d_{mean-EM}$ of constituent particles obtained by the three partners are consistent for three samples: relative deviations of 1% on TiO_2-LSSA, 2% on TiO_2 - µ-rutile, 5% on both the TiO_2-rods and the coated-TiO_2-E171. Therefore, the diameters $d_{mean-EM}$ and $d_{Feret-min-EM}$ were averaged, and the associated uncertainties used to calculate

the overall uncertainty (reproducibility variance) associated with the average values according to:

$$\sigma(d_{mean-EM}) = \frac{1}{3}\sqrt{\sum_{lab}\sigma^2(d_{mean-EM})_{lab}}$$

$\sigma^2(d_{mean-EM})_{lab}$ corresponds to a combination of the error related to particle sizing and the confidence interval of the gaussian fit described in section 2.2.1. A thorough methodology to determine the standard deviation on particle size determined from EM measurements is provided in a recent work from LNE [54]. For the three partners involved in particle sizing, the reproducibility variance is smaller than 10 nm.

3.2. Size characterization using the volume specific surface area

3.2.1. Comparison of the specific surface area of the four samples

The specific surface area (SSA) measurements evaluated by the BET model are shown in Figure 4 for all participants. The isotherms measured were categorized as type II (see Supporting Information), confirming the absence of particle porosity [55, 56].

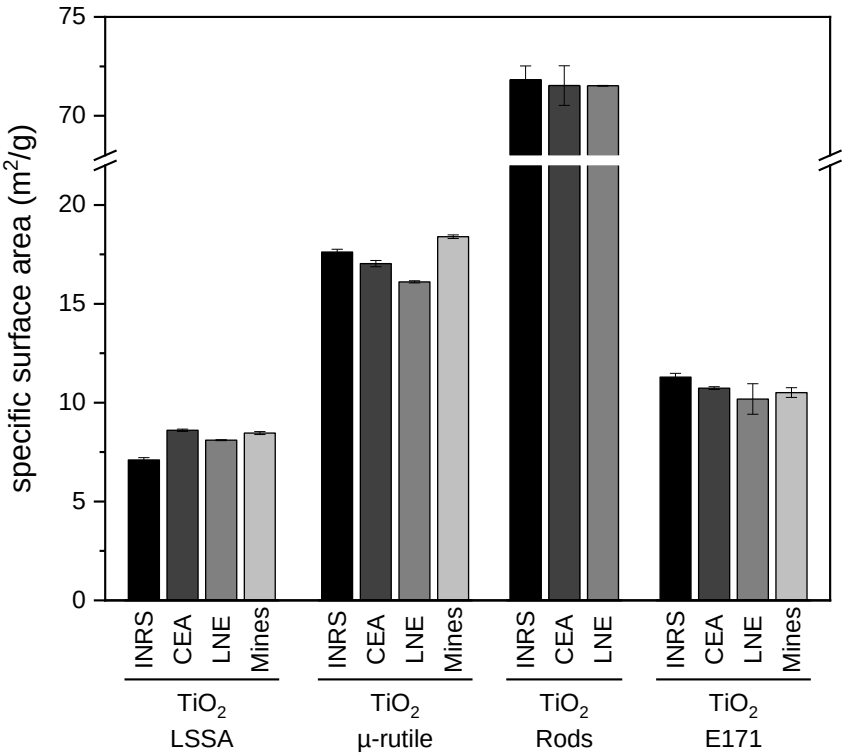

Figure 4. Specific surface area measured by gas adsorption and application of the BET model

A very good repeatability of measurements was obtained by each of the laboratories with variation coefficients found lower than 1.6% (all data combined). Furthermore, Fig. 4 highlights a fairly consistent reproducibility with low relative differences among the different partners, calculated according to:

$$\Delta = \frac{SSA_i - \overline{SSA}}{\overline{SSA}} \quad (6)$$

with SSA_i the specific surface area provided by partner i and $\overline{SSA}$ the mean specific surface area determined from the data of the three labs involved. The following values of Δ were obtained: 12% on the LSSA TiO_2 sample, 6% on the µ-rutile TiO_2 sample, 1% on the rod-type TiO_2 and 6% on the TiO_2 - E171. The reproducibility standard deviations were found equal to 0.04 m^2/g for TiO_2 – LSSA, 0.06 m^2/g for µ-rutile, 0.41 m^2/g for rods, and 0.21 m^2/g for E171. These observations are in line with previous work from Bau *et al.* [43] who state that *SSA* obtained by gas adsorption analysis is accurate within ± 15-20%.The averaged values of the specific surface area $\overline{SSA}$ were considered in the calculation of VSSA-based equivalent diameters.

3.2.2. Comparison of VSSA equivalent diameter and SEM assuming monodisperse constituent particles

An equivalent diameter $d_{mean-SSA}$ was calculated from VSSA data and equations (3) and (4). The results are compared to the mean diameter measured by EM $d_{mean-EM}$ assuming the particles are well dispersed and monodisperse in Table 3.

Table 3. Comparison of equivalent diameter obtained by EM and VSSA assuming monodisperse constituent particles. The values indicated in this Table were averaged from data obtained by all laboratories.

	TiO_2 - LSSA	**TiO_2 - µ-rutile**	**TiO_2 - Rods**	**TiO_2 - E171**
Shape	sphere	sphere	cylinder	sphere
Mean SSA (m^2/g)	8.1 ± 0.1	17.3 ± 0.1	71.6 ± 0.4	10.7 ± 0.2
Mean ρ_p (g/cm^3)	4.07 ± 0.11	4.15 ± 0.15	3.83 ± 0.01	3.96 ± 0.00
Mean VSSA (m^2/cm^3) – equation (1)	32.9 ± 0.9	71.8 ± 2.6	274.5 ± 1.7	42.3 ± 0.8
$d_{mean-SSA}$ (nm)	182.5 ± 5.2	83.6 ± 3.0	14.6 ± 0.1	141.9 ± 2.8
$d_{mean-EM}$ (nm)*	130.5 ± 4.0	224.3 ± 2.9	15.7 ± 0.1	100.1 ± 1.2
Relative discrepancy $\frac{d_{mean-SSA}-d_{mean-EM}}{d_{mean-EM}}$ (%)	40	-63	-7	42

* $d_{Feret-min-EM}$ for TiO_2 - Rods

Table 3 shows that the SSA of the four samples range from ~ 8 to ~ 70 m^2/g. The sample densities were obtained by He pycnometry at Mines, and by means of the alternative equipment carried out at CEA and INRS; the results were found to be similar to the reference values (see

Supporting Information), within ±7% for the two samples analyzed by three partners. The VSSA cover almost an order of magnitude, from ~ 30 to ~ 270 m^2/cm^3. The resulting equivalent particle diameters, $d_{mean-SSA}$, based on the assumption of monodisperse particle populations, range from 15 to ~ 180 nm. As detailed above, materials with a VSSA lower than 6 m^2/cm^3 are not considered as nanomaterials, according to the definition provided by EC [15]. On this basis, none of the samples involved in this study can be excluded of being a nanomaterial.

When compared to the diameters stemming from EM analysis ($d_{mean-EM}$), the values of $d_{mean-SSA}$ present relative discrepancies of -63% for TiO_2-µ-rutile, -7% for TiO_2 – Rods, +40% for TiO_2 – LSSA and +42% for TiO_2 - E171. For the two last samples, these differences can be partly due to particle aggregation. Indeed, contrary to agglomerates, constituent particles are partly merged within aggregates. Consequently, the surface area of the aggregate is lower than the sum of that of the constituent particles, resulting in a decrease of the VSSA. To account for partial fusion of constituent particles, the overlap coefficient C_{ov} has been used by some authors [28, 57-60]. The overall surface area is reduced by a term involving this coefficient as well as the number of constituent particles N_p within the aggregate:

$$SA = \left[\pi \sum\nolimits_{d_p} N(d_p) d_p^2\right] \cdot \left[1 - \phi C_{ov}\left(1 - \frac{1}{N_p}\right)\right]$$

In that case, the equivalent diameter deduced from VSSA is overestimated. It must also be kept in mind that aggregation may impact the dimensional measurements from imaging and analysis.

The relative high discrepancy (-63%) observed for TiO_2-µ-rutile sample could also be attributed to the surface roughness of this sample, which seems to have influenced its VSSA (particularly, its SSA). This roughness could originate from an element different from TiO_2, which questions the validity of the assumption that the substance is pure.

Besides, the data provided in Table 3 suggest that the assumption of monodisperse particles leads to a bias in the evaluation of constituent particle diameter. Indeed, constituent particle polydispersion (see Fig. 2 and 3) is intrinsic to the sample itself, and found to be around 30%. The effect of particle polydispersion was therefore further investigated.

3.2.3. Influence of polydispersion on VSSA equivalent diameters

To improve the robustness of the determination of the size of TiO_2 particles, polydispersion has been taken into account according to:

$$d_{mean-SSA-poly} = d_{mean-SSA} \cdot \theta \quad (7)$$

where θ is a correction factor introduced by Bau *et al.* [43] that reflects the fact that the VSSA of a polydisperse material is lower than the one of a monodisperse material with the same median diameter. In practice, assuming that constituent particle diameters are distributed according to a normal law results in the following equations:

$$\theta = \frac{1 + \left(\frac{\sigma}{d_{mean-EM}}\right)^2}{1 + 3\left(\frac{\sigma}{d_{mean-EM}}\right)^2} \quad (8)$$

for spherical particles [43], and:

$$\theta = \frac{1}{1 + \left(\frac{\sigma}{d_{Feret-min-EM}}\right)^2} \quad (9)$$

for cylindrical particles with $L \gg d$ (see Appendix for demonstration). Additional calculations were performed to state whether polydispersion of the length of rod-type particles shall also be considered. The results yielded negligible impact on the VSSA, lower than 10% as soon as $\frac{L}{d} > 5$.

The ratios $\sigma/d_{mean-EM}$ and $\sigma/d_{Feret-min-EM}$ obtained from EM data provided by each partner (Fig. 2 and 3) were averaged and used to calculate the polydispersion correction factors θ, yielding values of 0.85 for TiO_2 - E171 ($\sigma/d_{mean-EM}$ = 0.30), 0.86 for TiO_2 – LSSA ($\sigma/d_{mean-EM}$ = 0.30), and 0.87 for TiO_2 - µ-rutile ($\sigma/d_{mean-EM}$ = 0.28). For the sample with the rod-type shape TiO_2 – Rods ($\sigma/d_{Feret-min-EM}$ = 0.26), a value of 0.92 was found.

The VSSA-based equivalent diameters accounting for polydispersion $d_{mean-SSA-poly}$ are displayed in Figure 5 and summarized in Table 4.

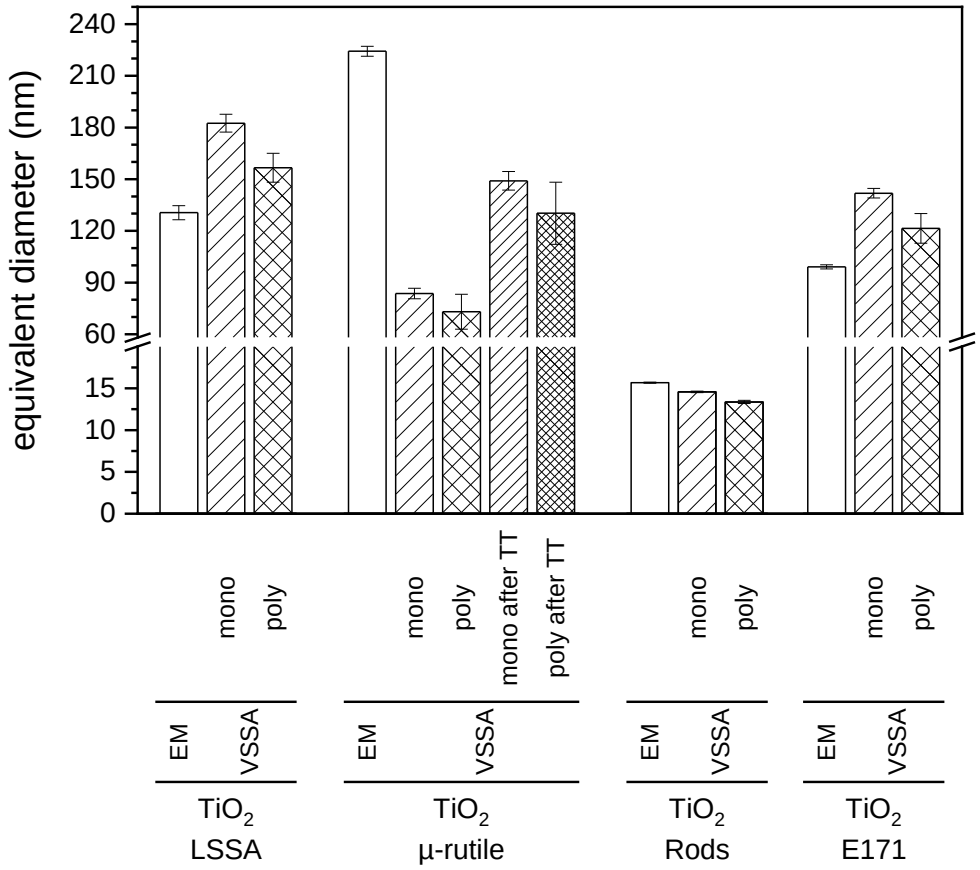

Figure 5. Comparison of EM ($d_{mean-EM}$) and VSSA-based ($d_{mean-SSA-poly}$) equivalent diameters for the four TiO_2 samples (after TT = after thermal treatment @ T=800°C). The values displayed correspond to averaged data obtained by all laboratories.

As expected, Figure 5 shows that accounting for polydispersion tends to decrease particle mean size (here, an average factor of 0.85 for spheres and 0.92 for cylinders was found). It can be observed from Fig. 5 and Table 4 that $d_{mean-SSA-poly}$ are in line with the diameters obtained from electron microscopy ($d_{mean-EM}$) within ± 20%, except for TiO_2 - µ-rutile sample (Table 4).

Though acceptable, the relative discrepancy obtained for TiO_2 – rods, is slightly larger when polydispersion is considered (-15%) than under the assumption of monodisperse particles (-7%). This may be due to a larger uncertainty in the determination of the size of constituent particles by electron microscopy. It is also worth noting that this difference corresponds to less than 3 nm in absolute value.

Table 4. Comparison of equivalent diameter obtained by EM and VSSA accounting for constituent particles polydispersion

	TiO_2 - LSSA	TiO_2 - µ-rutile	TiO_2 - Rods	TiO_2 - E171
Shape	sphere	sphere	cylinder	sphere
$\sigma/d_{mean-EM}$*	0.30 ± 0.02	0.28 ± 0.07	0.26 ± 0.04	0.31 ± 0.02
θ	0.86 ± 0.04	0.87 ± 0.12	0.92 ± 0.01	0.85 ± 0.03
$d_{mean-SSA-poly}$ (nm)	156.6 ± 8.4	73.0 ± 10.1	13.4 ± 0.2	120.6 ± 4.7
$d_{mean-EM}$ (nm)**	130.5 ± 4.0	224.3 ± 2.9	15.7 ± 0.1	100.1 ± 1.2
Relative discrepancy $\frac{d_{mean-SSA-poly}-d_{mean-EM}}{d_{mean-EM}}$ (%)	20	-67	-15	20

* $\sigma/d_{Feret-min-EM}$ for TiO_2 – Rods

** $d_{Feret-min-EM}$ for TiO_2 - Rods

To take into account polydispersion in the calculation of equivalent diameter, we have already stated that it is necessary to have a pure sample at the outset. The roughness of the particle surface greatly influences its VSSA.

For the specific case of TiO_2 - µ-rutile that presents the largest difference (-63% assuming monodisperse constituent particles, Table 3, -67% accounting for their polydispersion, Table 4), complementary investigations were performed. Indeed, TiO_2-µ-rutile appears to be coated with an unidentified organic phase (Fig. 1b). In that case, the underestimation of constituent particle diameter is likely related to an overestimation of the specific surface area of this sample. It was therefore legitimate to state whether surface chemistry and/or porosity could induce a bias in the determination of the SSA. To go in depth, additional thermal treatment (4 hours at 800°C) has been performed on TiO_2 - µ-rutile powder; this protocol attempted to remove the organic coating (Fig. 6).

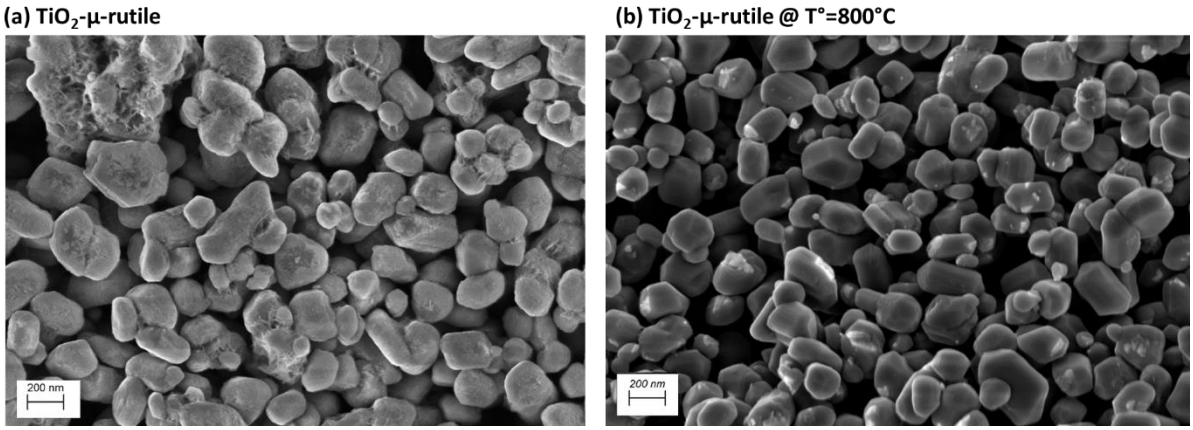

Figure 6. SEM images (a) Initial TiO_2 - µ-rutile and (b) TiO_2 - µ-rutile after thermal treatment @ T=800°C

Pre-treated TiO_2 - µ-rutile at 800°C was analysed by SEM to confirm the elimination of surface asperities. As it is clearly observed on SEM images (Fig. 6), this pre-treatment seems to remove the main compounds at the surface. Finally, the VSSA of sample TiO_2 - µ-rutile was almost divided by 2 after this thermal treatment, from 17.3 m^2/g to 9.7 m^2/g (Table 5). Thus, the equivalent diameter calculated for TiO_2 - µ-rutile after thermal treatment was increased and the bias between particle size from VSSA and the reference value obtained by microscopy decreased to -34% assuming monodisperse particles, and -42% considering polydispersion (Table 5).

Table 5. Comparison of equivalent diameter obtained by VSSA and SEM with TiO_2-µ-rutile sample before and after thermal treatment

	TiO_2-µ-rutile	**TiO_2-µ-rutile after calcination @ T=800°C**
Shape	sphere	sphere
Mean SSA (m^2/g)	17.3 ± 0.1	9.7 ± 0.0
Mean ρ_p (g/cm^3)*	4.15 ± 0.15	
Mean VSSA (m^2/cm^3)	71.8 ± 2.6	40.3 ± 1.5
$d_{mean-EM}$ (nm)	224.3 ± 2.9**	
$d_{mean-SSA}$ (nm)	83.6 ± 3.0	149.1 ± 5.4
$\frac{d_{mean-SSA}-d_{mean-EM}}{d_{mean-EM}}$ (%)	-63	-34
$d_{mean-SSA-poly}$ (nm)	73.0 ± 10.1	130.2 ± 18.0
$\frac{d_{mean-SSA-poly}-d_{mean-EM}}{d_{mean-EM}}$ (%)	-67	-42

* it is assumed that the density is similar after calcination

** no significant variation in particle size was observed after thermal treatment

Whether or not thermally treated, the isotherms obtained for this sample correspond to a non-porous material; applying the t-plot model [40] yields a fraction of surface related to microporosity lower than 10%. Therefore, the discrepancy between EM and VSSA-based diameters cannot be attributed to its porosity.

These complementary investigations support the fact that the determination of surface morphology is important. Furthermore, in this specific case, thermal treatment seems not to be sufficient. The presence of shiny particles at the TiO_2 interface in the SEM images (Fig. 6b) suggests the presence of another population that probably impacts VSSA values.

4. Conclusion

In this work, four samples of industrial or synthetized TiO_2 powder materials were considered. The characterization of the samples was performed by four partners involving complementary methods with the aim of producing data related to inter-laboratory reproducibility.

For each of the properties measured (i.e. the specific surface-area (Fig. 4), the bulk density (Supplementary Information, Fig. A), and the number size distribution (Fig. 2)), a satisfying agreement was observed between partners, in line with the literature. Electron microscopy, considered as the preferred method to determine the diameter of constituent particles, yielded values ranging from 15 to 225 nm.

Based on the volume specific surface area of the sample, the equivalent diameter of constituent particles was determined. This approach constitutes an interesting alternative to electron microscopy, since it relies on the combination of two straightforward analyses. Based on the assumptions that the sample is pure and consists in a single population, a VSSA-based equivalent diameter can be determined when the shape of constituent particles is known or supposed.

With the objective of improving the determination of the size of constituent particles, their polydispersion was considered through the introduction of a correction factor. The latter, which was first proposed in a previous work [43], is defined by means of geometric models, depending on particle shape, and hypothesis on the size distribution law. In this study, a normal size distribution was considered. Among the four TiO_2 investigated, a rod-type sample was introduced.

Except for one sample, the equivalent diameters derived from VSSA and including the correction factor related to polydispersion were found similar to the reference diameters from electron microscopy within ± 20%. Therefore, it is believed that this approach constitutes an interesting alternative methodology for estimating constituent particle diameter; further investigations involving more samples are still necessary. When the degree of polydispersion of the sample is unknown, a typical value of 30% can be considered as a first approximation, resulting in a correction factor of -15% ($\theta \approx 0.85$) for spherical particles.

Though future work involving more samples is still necessary, the approach involving polydispersion can be considered as an alternative methodology for estimating constituent particle diameter. It allows also state whether a material shall not be considered as a nanomaterial, as it has already been suggested by different authors [14, 37, 61-64]. In this alternative method, sample characterisation is carried out on a volume of powder larger than with microscopy, which limits potential bias due to sampling when the latter is very small.

Acknowledgments

The work has been performed in the frame of a French inter-laboratory comparison (ILC) exercise organised by the nanoMetrology Club (CnM). S. Bau would like to thank O. Rastoix from INRS for providing experimental data.

References

[1] HINCAPIÉ I., CABALLERO-GUZMAN A., HILTBRUNNER D., & NOWACK B. - Use of engineered nanomaterials in the construction industry with specific emphasis on paints and their flows in construction and demolition waste in Switzerland. *Waste management*, 2015, **43,** 398-406.

[2] KATZ L. M., DEWAN K., & BRONAUGH R. L. - Nanotechnology in cosmetics. *Food and Chemical Toxicology*, 2015, **85,** 127-137.

[3] PETERS R. J., BOUWMEESTER H., GOTTARDO S., AMENTA V., ARENA M., BRANDHOFF P., MARVIN H. J., MECH A., MONIZ F. B., & PESUDO L. Q. - Nanomaterials for products and application in agriculture, feed and food. *Trends in Food Science & Technology*, 2016, **54,** 155-164.

[4] PICCINNO F., GOTTSCHALK F., SEEGER S., & NOWACK B. - Industrial production quantities and uses of ten engineered nanomaterials in Europe and the world. *Journal of Nanoparticle Research*, 2012, **14,** 1-11.

[5] RECHES Y. - Nanoparticles as concrete additives: Review and perspectives. *Construction and Building Materials*, 2018, **175,** 483-495.

[6] KUIJPERS E., BEKKER C., BROUWER D., LE FEBER M., & FRANSMAN W. - Understanding workers' exposure: Systematic review and data-analysis of emission potential for NOAA. *Journal of Occupational and Environmental Hygiene*, 2017, **14,** 349-359.

[7] BEKKER C., KUIJPERS E., BROUWER D. H., VERMEULEN R., & FRANSMAN W. - Occupational exposure to nano-objects and their agglomerates and aggregates across various life cycle stages; a broad-scale exposure study. *Annals of Occupational Hygiene*, 2015**,** doi: 10.1093/annhyg/mev1023.

[8] BROUWER D. - Exposure to manufactured nanoparticles in different workplaces. *Toxicology*, 2010, **269,** 120-127.

[9] DEBIA M., BAKHIYI B., OSTIGUY C., VERBEEK J. H., BROUWER D. H., & MURASHOV V. - A Systematic Review of Reported Exposure to Engineered Nanomaterials. *The Annals of Occupational Hygiene*, 2016, **60,** 916-935.

[10] DING Y., KUHLBUSCH T. A., VAN TONGEREN M., JIMÉNEZ A. S., TUINMAN I., CHEN R., ALVAREZ I. L., MIKOLAJCZYK U., NICKEL C., & MEYER J. - Airborne engineered nanomaterials in the workplace—a review of release and worker exposure during nanomaterial production and handling processes. *Journal of hazardous materials*, 2017, **322,** 17-28.

[11] ZIMMERMANN E., DERROUGH S., LOCATELLI D., DURAND C., FROMAGET J. L., LEFRANC E., RAVANEL X., & GARRIONE J. - Results of potential exposure assessments during the maintenance and cleanout of deposition equipment. *Journal of Nanoparticle Research*, 2012, **14,** 1209.

[12] KUHLBUSCH T., ASBACH C., FISSAN H., GÖHLER D., & STINTZ M. - Nanoparticle exposure at nanotechnology workplaces: A review. *Particle and Fiber Toxicology*, 2011, **8,** 22.
[13] O'SHAUGHNESSY P. T. - Occupational health risk to nanoparticulate exposure. *Environmental Science: Processes & Impacts*, 2013, **15,** 49-62.
[14] MECH A., WOHLLEBEN W., GHANEM A., HODOROABA V. D., WEIGEL S., BABICK F., BRÜNGEL R., FRIEDRICH C. M., RASMUSSEN K., & RAUSCHER H. - Nano or Not Nano? A Structured Approach for Identifying Nanomaterials According to the European Commission's Definition. *Small*, 2020, **16,** 2002228.
[15] EUROPEAN COMMISSION - Commission recommendation of 10 June 2022 on the definition of nanomaterial. *Off. J. Eur. Union*, 2022, **65,** 2022/C 2229/2001.
[16] ANSES - Registre R-Nano. Evaluation des potentialités d'exploitation et de partage des données déclarées. Avis de l'Anses. Rapport d'expertise collective. 2020.
[17] RAUSCHER H., ROEBBEN G., AMENTA V., BOIX S., CALZOLAI L., EMONS H., GAILLARD C., GIBSON P., LINSINGER T., & MECH A. - Towards a Review of the EC Recommendation for a Definition of the Term "Nanomaterial". *Science and Policy Report by the Joint Research Centre of the European Commission, European Union*, 2014.
[18] BOVERHOF D. R., BRAMANTE C. M., BUTALA J. H., CLANCY S. F., LAFRANCONI M., WEST J., & GORDON S. C. - Comparative assessment of nanomaterial definitions and safety evaluation considerations. *Regulatory Toxicology and Pharmacology*, 2015, **73,** 137-150.
[19] RAUSCHER H., MECH A., GIBSON N., GILLILAND D., HELD A., KESTENS V., KOEBER R., LINSINGER T., & STEFANIAK E. - Identification of nanomaterials through measurements. *Publications Office of the European Union*, 2019**,** doi: 10.2760/053982.
[20] GAILLARD C., MECH A., WOHLLEBEN W., BABICK F., HODOROABA V.-D., GHANEM A., WEIGEL S., & RAUSCHER H. - A technique-driven materials categorisation scheme to support regulatory identification of nanomaterials. *Nanoscale Advances*, 2019, **1,** 781-791.
[21] WARHEIT D. B. - Hazard and risk assessment strategies for nanoparticle exposures: how far have we come in the past 10 years? *F1000 Research*, 2018, **7,** 376.
[22] WARHEIT D. B. & DONNER E. M. - Risk assessment strategies for nanoscale and fine-sized titanium dioxide particles: Recognizing hazard and exposure issues. *Food and Chemical Toxicology*, 2015, **85,** 138-147.
[23] WANG J., ASBACH C., FISSAN H., HÜLSER T., KUHLBUSCH T. A. J., THOMPSON D., & PUI D. Y. H. - How can nanobiotechnology oversight science and industry: examples from environmental, health, and safety studies of nanoparticles (nano-EHS). *Journal of Nanoparticle Research*, 2011, **13,** 1373-1387.
[24] POWERS K. W., PALAZUELOS M., MOUDGIL B. M., & ROBERTS S. M. - Characterization of the size, shape, and state of dispersion of nanoparticles for toxicological studies. *Nanotoxicology*, 2007, **1,** 42-51.
[25] NASTERLACK M., ZOBER A., & OBERLINNER C. - Considerations on occupational medical surveillance in employees handling nanoparticles. *International archives of occupational and environmental health*, 2008, **81,** 721-726.
[26] SCHULTE P. A., SCHUBAUER-BERIGAN M. K., MAYWEATHER C., GERACI C. L., ZUMWALDE R., & MCKERNAN J. L. - Issues in the Development of Epidemiologie Studies of Workers Exposed to Engineered Nanoparticles. *Journal of Occupational and Environmental Medicine*, 2009**,** 323-335.

584 [27] MAVROCORDATOS D., PERRET D., & LEPPARD G. G. - Strategies and advances
585 in the characterisation of environmental colloids by electron microscopy. *IUPAC*
586 *SERIES ON ANALYTICAL AND PHYSICAL CHEMISTRY OF ENVIRONMENTAL*
587 *SYSTEMS*, 2007, **10,** 345.
588 [28] BAU S., WITSCHGER O., GENSDARMES F., RASTOIX O., & THOMAS D. - A
589 TEM-based method as an alternative to the BET method for measuring off-line the
590 specific surface-area of nanoaerosols. *Powder Technology*, 2010, **200,** 190-201.
591 [29] FAVRE G., FELTIN N., & BAU S. - Mesure de la taille de nanoparticules : retour sur
592 une comparaison inter-laboratoires et inter-techniques. *Hygiène et Sécurité du Travail*,
593 2020, **260,** 60-67.
594 [30] DAZON C., MAXIT B., & WITSCHGER O. - Comparison between a low-voltage
595 benchtop electron microscope and conventional TEM for number size distribution of
596 nearly spherical shape constituent particles of nanomaterial powders and colloids.
597 *Micron*, 2019, **116,** 124-129.
598 [31] KREYLING W. G., SEMMLER-BEHNKEA M., & CHAUDHRYB Q. - A
599 complementary definition of nanomaterials. *Nano Today*, 2010, **5,** 165-168.
600 [32] DAZON C., WITSCHGER O., BAU S., FIERRO V., & LLEWELLYN P. L. - Toward
601 an operational methodology to identify industrial-scaled nanomaterial powders with the
602 volume specific surface area criterion. *Nanoscale Advances*, 2019, **1,** 3232-3242.
603 [33] LECLOUX A. J. - Discussion about the use of the volume-specific surface area (VSSA)
604 as criteria to identify nanomaterials according to the EU definition. *Journal of*
605 *Nanoparticle Research*, 2015, **17,** 447.
606 [34] LECLOUX A. J., ATLURI R., KOLEN'KO Y. V., & DEEPAK F. L. - Discussion about
607 the use of the volume specific surface area (VSSA) as a criterion to identify
608 nanomaterials according to the EU definition. Part two: experimental approach.
609 *Nanoscale*, 2017, **9,** 14952-14966.
610 [35] BABICK F., MIELKE J., WOHLLEBEN W., WEIGEL S., & HODOROABA V.-D. -
611 How reliably can a material be classified as a nanomaterial? Available particle-sizing
612 techniques at work. *Journal of Nanoparticle Research*, 2016, **18,** 158.
613 [36] SCENIHR - Scientific Basis for the Definition of the Term "nanomaterial"
614 *http://ec.europa.eu/health/scientific_committees/emerging/docs/scenihr_o_032.pdf*,
615 2010.
616 [37] WOHLLEBEN W., MIELKE J., BIANCHIN A., GHANEM A., FREIBERGER H.,
617 RAUSCHER H., GEMEINERT M., & HODOROABA V.-D. - Reliable nanomaterial
618 classification of powders using the volume-specific surface area method. *Journal of*
619 *Nanoparticle Research*, 2017, **19,** 61.
620 [38] DAZON C., FIERRO V., CELZARD A., & WITSCHGER O. - Identification of
621 nanomaterials by the volume specific surface area (VSSA) criterion: application to
622 powder mixes. *Nanoscale Advances*, 2020, **2,** 4908-4917.
623 [39] BRUNAUER S., EMMETT P. H., & TELLER E. - Adsorption of gases in
624 multimolecular layers. *Journal of the American chemical society*, 1938, **60,** 309-319.
625 [40] LIPPENS B. C. & DE BOER J. - Studies on pore systems in catalysts: V. The t method.
626 *Journal of Catalysis*, 1965, **4,** 319-323.
627 [41] LOWELL S., SHIELDS J. E., THOMAS M. A., & THOMMES M. (2006)
628 *Characterization of porous solids and powders: surface area, pore size and density*
629 (Springer Science & Business Media).
630 [42] GIBSON N., RAUSCHER H., & ROEBBEN G. - Comments on the article by AJ
631 Lecloux (J Nanopart Res (2015) 17: 447) regarding the use of volume-specific surface
632 area (VSSA) to classify nanomaterials. *Journal of Nanoparticle Research*, 2016, **18,** 1-
633 8.

[43] BAU S., DAZON C., RASTOIX O., & BARDIN-MONNIER N. - Effect of constituent particle polydispersion on VSSA-based equivalent particle diameter: Theoretical rationale and application to a set of eight powders with constituent particle median diameters ranging from 9 to 130 nm. *Advanced Powder Technology*, 2021, **32,** 1369-1379.
[44] BOUZAKHER-GHOMRASNI N., TACHE O., LEROY J., FELTIN N., TESTARD F., & CHIVAS-JOLY C. - Dimensional measurement of TiO2 (Nano) particles by SAXS and SEM in powder form. *Talanta*, 2021, **234,** 122619.
[45] BRESCH H., HODOROABA V.-D., SCHMIDT A., RASMUSSEN K., & RAUSCHER H. - Counting Small Particles in Electron Microscopy Images—Proposal for Rules and Their Application in Practice. *Nanomaterials*, 2022, **12,** 2238.
[46] GHOMRASNI N. B., CHIVAS-JOLY C., DEVOILLE L., HOCHEPIED J.-F., & FELTIN N. - Challenges in sample preparation for measuring nanoparticles size by scanning electron microscopy from suspensions, powder form and complex media. *Powder Technology*, 2020, **359,** 226-237.
[47] DE TEMMERMAN P.-J., VERLEYSEN E., LAMMERTYN J., & MAST J. - Semi-automatic size measurement of primary particles in aggregated nanomaterials by transmission electron microscopy. *Powder Technology*, 2014, **261,** 191-200.
[48] DE TEMMERMAN P.-J., VAN DOREN E., VERLEYSEN E., VAN DER STEDE Y., FRANCISCO M. A. D., & MAST J. - Quantitative characterization of agglomerates and aggregates of pyrogenic and precipitated amorphous silica nanomaterials by transmission electron microscopy. *Journal of Nanobiotechnology*, 2012, **10,** 24.
[49] VERLEYSEN E., DE TEMMERMAN P. J., VAN DOREN E., ABI DAOUD FRANCISCO M., & MAST J. - Quantitative characterization of aggregated and agglomerated titanium dioxide nanomaterials by transmission electron microscopy. *Powder Technology*, 2014, **258,** 180-188.
[50] TERRELL G. R. & SCOTT D. W. - Oversmoothed Nonparametric Density Estimates. *Journal of the American Statistical Association*, 1985, **80,** 209-214.
[51] OLSON E. - The importance of sample preparation when measuring specific surface area. *Journal of GXP Compliance*, 2012, **16,** 52-62.
[52] ISO - ISO 15901-2: Pore size distribution and porosity of solid materials by mercury porosimetry and gas adsorption — Part 2: Analysis of nanopores by gas adsorption. 2022.
[53] ISO - ISO 9277: Determination of the specific surface area of solids by gas adsorption — BET method. 2022.
[54] FELTIN N., DELVALLÉE A., & CROUZIER L. - Strategy for Ensuring the Metrological Traceability of Nanoparticle Size Measurements by SEM. *Nanomaterials*, 2024, **14,** 931.
[55] THOMMES M., KANEKO K., NEIMARK A. V., OLIVIER J. P., RODRIGUEZ-REINOSO F., ROUQUEROL J., & SING K. S. W. - Physisorption of gases, with special reference to the evaluation of surface area and pore size distribution (IUPAC Technical Report). *Pure and Applied Chemistry*, 2015, **87,** 1051-1069.
[56] SING K. S. - Reporting physisorption data for gas/solid systems with special reference to the determination of surface area and porosity (Recommendations 1984). *Pure and Applied Chemistry*, 1985, **57,** 603-619.
[57] BRASIL A. M., FARIAS T. L., & CARVALHO M. G. - A recipe for image characterization of fractal-like aggregates. *J Aerosol Sci*, 1999, **30**.
[58] GWAZE P., SCHMID O., ANNEGARN H. J., ANDREAE M. O., HUTH J., & HELAS G. - Comparison of three methods of fractal analysis applied to soot aggregates from wood combustion. *Journal of Aerosol Science*, 2006, **37,** 820-838.

[59] BOURROUS S., RIBEYRE Q., LINTIS L., YON J., BAU S., THOMAS D., VALLIÈRES C., & OUF F.-X. - A semi-automatic analysis tool for the determination of primary particle size, overlap coefficient and specific surface area of nanoparticles aggregates. *Journal of Aerosol Science*, 2018, **126,** 122-132.

[60] OH C. & SORENSEN C. M. - The effect of overlap between monomers on the determination of fractal cluster morphology. *Journal of Colloid and Interface Science*, 1997, **193,** 17-25.

[61] BRÜNGEL R., RÜCKERT J., MÜLLER P., BABICK F., FRIEDRICH C. M., GHANEM A., HODOROABA V.-D., MECH A., WEIGEL S., & WOHLLEBEN W. - NanoDefiner Framework and e-Tool Revisited According to the European Commission's Nanomaterial Definition 2022/C 229/01. *Nanomaterials*, 2023, **13,** 990.

[62] BRÜNGEL R., RÜCKERT J., WOHLLEBEN W., BABICK F., GHANEM A., GAILLARD C., MECH A., RAUSCHER H., HODOROABA V.-D., WEIGEL S., & FRIEDRICH C. M. - NanoDefiner e-Tool: An Implemented Decision Support Framework for Nanomaterial Identification. *Materials*, 2019, **12,** 3247.

[63] DAZON C., WITSCHGER O., BAU S., FIERRO V., & LLEWELLYN P. - Classification of nanoparticles in powder form: comparing VSSA, XRD and SEM. *Environmental Science: Nano*, 2019, **6,** 152-162.

[64] DAZON C., WITSCHGER O., BAU S., FIERRO V., & LLEWELLYN P. - Toward an operational methodology to identify industrial-scaled nanomaterial powders with the Volume Specific Surface Area criterion. *Nanoscale Advances*, 2019, **1,** 3232-3242.

Appendix: Demonstration of the expression of the VSSA of rod-type particles whose diameter is distributed according to a normal law with parameters d_m, σ (mean diameter and standard deviation, respectively)

The cylinder length is noted L and its diameter d. It is assumed that $L \gg d$.

The surface-area of a cylinder is given by:

$$SA = \frac{\pi d^2}{2} + \pi dL$$

and can be approximated by ($L \gg d$):

$$SA \approx \pi dL$$

The volume of a cylinder is expressed according to:

$$V = \frac{\pi d^2}{4} L$$

The Volume Specific Surface Ara is therefore, assuming monodisperse particles with diameter d:

$$VSSA_{mono} = \frac{SA}{V} = \frac{\pi dL}{\frac{\pi}{4} d^2 L} = \frac{4}{d}$$

Considering polydisperse constituent particle diameter yields:

$$VSSA_{poly} = \frac{\sum_d SA}{\sum_d V} = \frac{\sum_d \pi dL}{\sum_d \frac{\pi}{4} d^2 L}$$

Or:

$$VSSA_{poly} = \frac{\int_d N(d) \pi dL}{\int_d N(d) \frac{\pi}{4} d^2 L}$$

Under the assumption of a normal distribution of the diameter of constituent particles $N(d)$, the last equation can be written:

$$VSSA_{poly} = \frac{\int_{d_{min}}^{d_{max}} \exp\left[-\frac{1}{2}\left(\frac{d - d_m}{\sigma}\right)^2\right] \pi dL \mathrm{d}d}{\int_{d_{min}}^{d_{max}} \exp\left[-\frac{1}{2}\left(\frac{d - d_m}{\sigma}\right)^2\right] \frac{\pi}{4} d^2 L \mathrm{d}d}$$

which simplifies as:

$$VSSA_{poly} = 4 \frac{\int_{d_{min}}^{d_{max}} \exp\left[-\frac{1}{2}\left(\frac{d - d_m}{\sigma}\right)^2\right] d \mathrm{d}d}{\int_{d_{min}}^{d_{max}} \exp\left[-\frac{1}{2}\left(\frac{d - d_m}{\sigma}\right)^2\right] d^2 \mathrm{d}d} = 4 \frac{I_1}{I_2}$$

with:

$$I_1 = \int_{d_{min}}^{d_{max}} \exp\left[-\frac{1}{2}\left(\frac{d-d_m}{\sigma}\right)^2\right] d\mathrm{d}d$$

$$I_2 = \int_{d_{min}}^{d_{max}} \exp\left[-\frac{1}{2}\left(\frac{d-d_m}{\sigma}\right)^2\right] d^2\mathrm{d}d$$

As the integration is performed over the whole range of diameters supposed to be normally distributed ($d_{min} = d_m - k.\sigma$ and $d_{max} = d_m + k.\sigma$), the following transformation of integration variable is operated:

$$x = \frac{d-d_m}{\sigma}$$

leading to these changes for the variable and the limits:

$$\mathrm{d}d = \sigma.\mathrm{d}x$$

$$x_{min} = -k$$

$$x_{max} = +k$$

Let us consider the case of I_1:

$$I_1 = \int_{-k}^{k} \exp\left(-\frac{x^2}{2}\right)(\sigma x + d_m)\sigma.\mathrm{d}x$$

$$I_1 = \int_{-k}^{k} \sigma^2 x \exp\left(-\frac{x^2}{2}\right)\mathrm{d}x + \int_{-k}^{k} \sigma d_m \exp\left(-\frac{x^2}{2}\right)\mathrm{d}x$$

Due to the parity properties of the functions in this expanded expression of I_1, equation can be simplified as:

$$I_1 = 2\sigma d_m \int_{0}^{k} \exp\left(-\frac{x^2}{2}\right)\mathrm{d}x$$

Because:

$$\int_{0}^{k} \exp\left(-\frac{x^2}{2}\right)\mathrm{d}x = \sqrt{\frac{\pi}{2}}\,\mathrm{erf}\left(\frac{k}{\sqrt{2}}\right) \approx \sqrt{\frac{\pi}{2}}$$

Finally, this yields:

$$I_1 = \sigma d_m \sqrt{2\pi}$$

The second integral I_2can be evaluated in a similar manner:

$$I_2 = \sigma\left[\int_{-k}^{k} \sigma^2 x^2 \exp\left(-\frac{x^2}{2}\right) dx + \int_{-k}^{k} 2\sigma x d_m \exp\left(-\frac{x^2}{2}\right) dx + \int_{-k}^{k} d_m^2 \exp\left(-\frac{x^2}{2}\right) dx\right]$$

Which can be simplified as:

$$I_2 = \sigma\left[2\sigma^2 \int_{0}^{k} x^2 \exp\left(-\frac{x^2}{2}\right) dx + 0 + 2d_m^2 \int_{0}^{k} \exp\left(-\frac{x^2}{2}\right) dx\right]$$

$$I_2 = \sigma\left[2\sigma^2\sqrt{\frac{\pi}{2}} + 2d_m^2\sqrt{\frac{\pi}{2}}\right]$$

$$I_2 = \sigma\sqrt{2\pi}\,(\sigma^2 + d_m^2)$$

Therefore:

$$VSSA_{poly} = \frac{4d_m}{\sigma^2 + d_m^2} = VSSA_{mono}\left[\frac{1}{1 + \left(\frac{\sigma}{d_m}\right)^2}\right]$$

Which can be also written in terms of correction factor:

$$\theta = \frac{1}{1 + \left(\frac{\sigma}{d_m}\right)^2}$$

Supplemental Information

Figure A presents the values of sample density obtained:

- by He pycnometry for laboratory “Mines”
- an alternative method based on gas adsorption for both laboratories “INRS” and “CEA”.

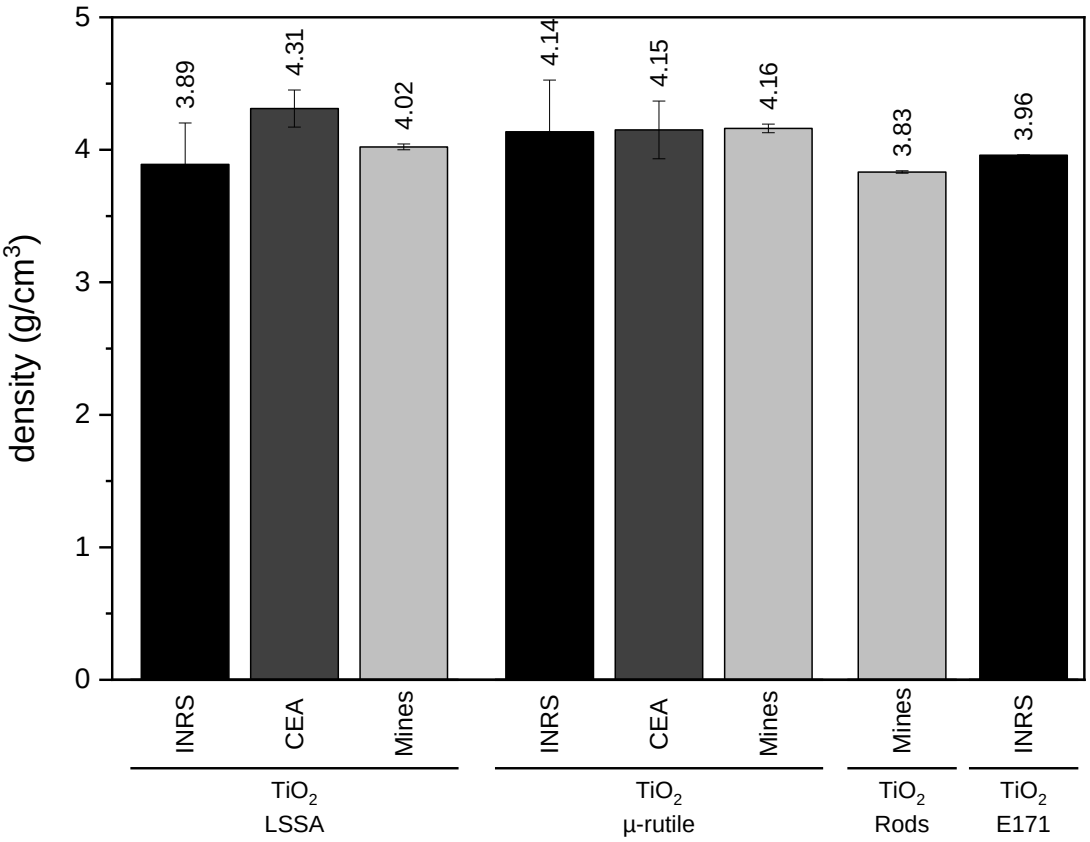

Figure A. Comparison of sample density.

The isotherms obtained from gas adsorption measurements are displayed in Figure B for the four TiO_2 samples considered in this study.

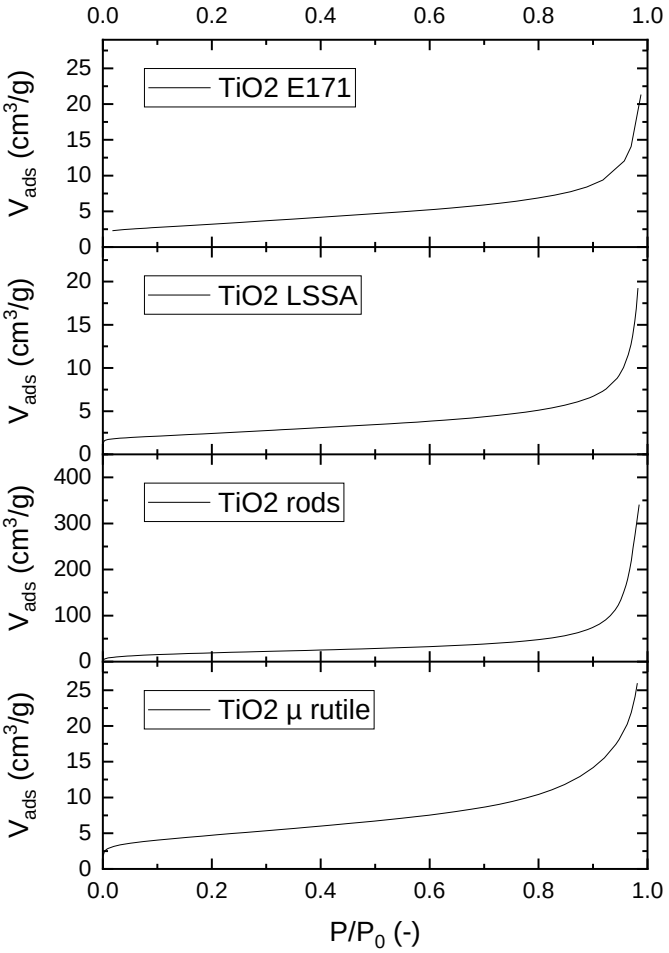

780

781 Figure B. Gas adsorption isotherms (N_2 at 77.4K) of the four TiO_2 samples.

782